Journal of Organometallic Chemistry, 450 (1993) 157–164

JOM 23280

Structures of propionaldehyde, butyraldehyde, and pivalaldehyde complexes of the chiral rhenium fragment $[(\eta^5\text{-}C_5H_5)Re(NO)(PPh_3)]^+$

Darryl P. Klein, N. Quirós Méndez, Jeffery W. Seyler, Atta M. Arif and J.A. Gladysz

Department of Chemistry, University of Utah, Salt Lake City, UT 84112 (USA)

(Received July 27, 1992; in revised form October 5, 1992)

Abstract

The crystal structures of propionaldehyde complex (*RS,SR*)-$[(\eta^5\text{-}C_5H_5)Re(NO)(PPh_3)(\eta^2\text{-}O{=}CHCH_2CH_3)]^+$ PF_6^- (**1b**$^+$ PF_6^-; monoclinic, $P2_1/c$ (No. 14), $a = 10.166(1)$ Å, $b = 18.316(1)$ Å, $c = 14.872(2)$ Å, $\beta = 100.51(1)°$, $Z = 4$) and butyraldehyde complex (*RS,SR*)-$[(\eta^5\text{-}C_5H_5)Re(NO)(PPh_3)(\eta^2\text{-}O{=}CHCH_2CH_2CH_3)]^+$ PF_6^- (**1c**$^+PF_6^-$; monoclinic, $P2_1/a$ (No. 14), $a = 14.851(1)$ Å, $b = 18.623(3)$ Å, $c = 10.026(2)$ Å, $\beta = 102.95(1)°$, $Z = 4$) have been determined at 22°C and −125°C, respectively. These exhibit C⎓O bond lengths (1.35(1), 1.338(5) Å) that are intermediate between those of propionaldehyde (1.209(4) Å) and 1-propanol (1.41 Å). Other geometric features are analyzed. Reaction of $[(\eta^5\text{-}C_5H_5)Re(NO)(PPh_3)(ClCH_2Cl)]^+$ BF_4^- and pivalaldehyde gives $[(\eta^5\text{-}C_5H_5)Re(NO)(PPh_3)(\eta^2\text{-}O{=}CHC(CH_3)_3)]^+BF_4^-$ (81%), the spectroscopic properties of which establish a π C⎓O binding mode.

1. Introduction

Many enantioselective transformations of aldehydes and ketones involve some type of bonding interaction with a chiral Lewis acid species [1–3]. Accordingly, a detailed understanding of aldehyde–Lewis acid binding modes and dynamic behavior is essential for analysis of the mechanisms of asymmetric induction. Hence, we have undertaken an extensive study of the structural, dynamic, and chemical properties of adducts of organic carbonyl compounds and the chiral rhenium fragment $[(\eta^5\text{-}C_5H_5)Re(NO)(PPh_3)]^+$ (**I**) [4–10]. Other researchers have initiated parallel experimental and theoretical efforts utilizing different types of Lewis acids [11,12].

All aliphatic aldehyde complexes of **I** examined to date adopt the idealized ground state π binding mode **II** shown in Chart 1 [5]. The stereoelectronic basis for this preference has been previously analyzed in detail [5]. However, *ca.* 1% of another diastereomer, **III**, can in some cases be detected in solution by low temperature NMR (R = **a**, CH_3; **d**, $CH(CH_3)_2$) [7b]. Isomers **II** and **III** differ in the C=O enantioface that binds to the chiral rhenium fragment, and can be distinguished by *R/S* nomenclature conventions detailed earlier [5]. For convenience, the C=O alkyl substituents are designated by the same indices (**a**, **b**, *etc.*) employed in a preceding paper [5].

We have previously determined the crystal structures of two aliphatic aldehyde complexes, the propionaldehyde complex (*RS,SR*)-$[(\eta^5\text{-}C_5H_5)Re(NO)(PPh_3)(\eta^2\text{-}O{=}CHCH_2CH_3)]^+$ BF_4^- (**1b**$^+$ BF_4^-) and phenylacetaldehyde complex (*RS,SR*)-$[(\eta^5\text{-}C_5H_5)Re(NO)(PPh_3)(\eta^2\text{-}O{=}CHCH_2C_6H_5)]^+$ PF_6^- (**1f**$^+$ PF_6^-) [5]. However, the ethyl group in the former was disordered, giving two OC–CH_2R′ rotamers in the solid state. As more structural data on this class of compounds became available, we began to suspect that the metrical parameters associated with the Re–(O⎓C) moiety in **1b**$^+$ BF_4^- were unreliable. As part of an effort to correlate aldehyde and alkene [13] enantioface binding selectivities to structural features, it was essential to have accurate baseline data for complexes of **I** and simple aliphatic aldehydes. Thus, we set out to acquire X-ray diffraction data on closely related compounds in which disorder would hopefully be avoided.

In this paper, we report the crystal structures of the propionaldehyde complex (*RS,SR*)-$[(\eta^5\text{-}C_5H_5)Re(NO)(PPh_3)(\eta^2\text{-}O{=}CHCH_2CH_3)]^+$ PF_6^- (**1b**$^+$ PF_6^-)

Correspondence to: Prof. J.A. Gladysz.

0022-328X/93/$6.00

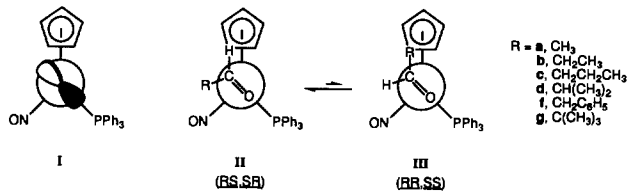

Chart 1. **I**: Pyramidal rhenium fragment $[(\eta^5\text{-}C_5H_5)Re(NO)(PPh_3)]^+$ with d-orbital HOMO; **II** and **III**: Newman projections of possible diastereomers of aldehyde complexes $[(\eta^5\text{-}C_5H_5)Re(NO)(PPh_3)(\eta^2\text{-}O{=}CHR)]^+ X^-$ ($\mathbf{1}^+ X^-$).

and butyraldehyde complex (*RS,SR*)-$[(\eta^5\text{-}C_5H_5)Re(NO)(PPh_3)(\eta^2\text{-}O{=}CHCH_2CH_2CH_3)]^+ PF_6^-$ ($\mathbf{1c}^+ PF_6^-$). We also describe the synthesis of the corresponding pivalaldehyde complex, and spectroscopic data that indicate that despite the additional ligand bulk, the π binding mode greatly predominates in solution.

2. Results

2.1. Crystal structures

Samples of $\mathbf{1b}^+ PF_6^-$ and $\mathbf{1c}^+ PF_6^-$ were obtained as described previously [5], or from the corresponding tetrafluoroborate salts by a counter-anion metathesis procedure. X-ray data were collected at room temperature for $\mathbf{1b}^+ PF_6^-$ and −125°C for $\mathbf{1c}^+ PF_6^-$ as summarized in Table 1. Refinement, described in the Experimental section, gave the structures shown in Figs. 1 and 2. The O⎓CH hydrogen atoms were located, and that of $\mathbf{1c}^+ PF_6^-$ was refined. Except for the PF_6^- anion in $\mathbf{1b}^+ PF_6^-$, no disorder was observed.

TABLE 1. Summary of crystallographic data for aliphatic aldehyde complexes (*RS,SR*)-$[(\eta^5\text{-}C_5H_5)Re(NO)(PPh_3)(\eta^2\text{-}O{=}CHCH_2CH_3)]^+ PF_6^-$ ($\mathbf{1b}^+ PF_6^-$) and (*RS,SR*)-$[(\eta^5\text{-}C_5H_5)Re(NO)(PPh_3)(\eta^2\text{-}O{=}CHCH_2CH_2CH_3)]^+ PF_6^-$ ($\mathbf{1c}^+ PF_6^-$)

	$\mathbf{1b}^+ PF_6^-$	$\mathbf{1c}^+ PF_6^-$
Molecular formula	$C_{26}H_{26}F_6NO_2P_2Re$	$C_{27}H_{28}F_6NO_2P_2Re$
Molecular weight	746.641	760.668
Crystal system	monoclinic	monoclinic
Space group	$P2_1/c$ (No. 14)	$P2_1/a$ (No. 14) [a]
Cell dimensions		
a, Å	10.166(1)	14.851(1)
b, Å	18.316(1)	18.623(3)
c, Å	14.872(2)	10.026(2)
β, deg	100.51(1)	102.95(1)
V, Å^3	2722.71	2702.30
Z	4	4
Temp, °C	22	−125
d_{calc}, g cm^{-3}	1.82	1.87
d_{obs}, g cm^{-3} (CCl_4/CH_2I_2)	1.80 (25°C)	1.80 (25°C)
Crystal dimensions, mm	0.25 × 0.19 × 0.09	0.31 × 0.24 × 0.09
Diffractometer	Enraf-Nonius CAD-4	Enraf-Nonius CAD-4
Radiation (λ, Å)	Cu Kα (1.54056)	Cu Kα (1.54056)
Data collection method	θ–2θ	θ–2θ
Scan speed, deg/min	variable, 1–8	variable, 1–8
Reflections measured	4983	4333
Range/indices (hkl)	0,11 0,21 − 17,17	0,16 0,20 − 11,11
Scan range	0.80 + 1.40 (tan θ)	0.80 + 1.40 (tan θ)
2θ limit, deg	4.0-130.0	4.0-130.0
Time between std	1 X-ray hour	1 X-ray hour
Total no. of unique data	4790	4008
No. of observed data, $I > 3\sigma(I)$	3536	3620
Abs coefficient, cm^{-1}	101.44	102.33
Min transmission, %	48.11	33.24
Max transmission, %	99.90	98.58
No. of variables	343	355
Goodness of fit	1.10	2.01
R (averaging) (I_{obs}, F_{obs})	0.021, 0.018	0.027, 0.016
$R = \Sigma \lvert\lvert F_o \rvert - \lvert F_c \rvert\rvert / \Sigma \lvert F_o \rvert$	0.043	0.032
$R_w = \Sigma \lvert\lvert F_o \rvert - \lvert F_c \rvert\rvert w^{1/2} / \Sigma \lvert F_o \rvert w^{1/2}$	0.052	0.046
Δ/σ (max)	0.014	0.001
$\Delta\rho$ (max), e Å^{-3}	1.103 (1.1 Å from F4)	1.163 (1.6 Å from Re)

[a] Nonstandard setting of $P2_1/c$.

Atomic coordinates, and selected bond lengths, bond angles, and torsion angles, are given in Tables 2 and 3.

As is shown in Figs. 1 and 2, **1b**, $\mathbf{c}^+$ PF_6^- adopt Re–(O⋯C) conformations close to that of the idealized structure **II** (Chart 1). The moderate difference was analyzed in several ways. For example, the Re–P and Re–N bonds in **II** make angles of 0° and 90°, respectively, with the Re–O⋯C plane. In $\mathbf{1b}^+$ PF_6^-, the corresponding angles were found to be 17.0° and 69.8°. In $\mathbf{1c}^+$ PF_6^-, these angles were 20.5° and 69.5°. Alternatively, the angles of the Re–O⋯C planes with the planes defined by Re–P bonds and the C⋯O midpoints were calculated ($\mathbf{1b}^+$ PF_6^-: 17.2°, 72.0°; $\mathbf{1c}^+$ PF_6^-: 20.6°, 71.4°). These closely matched the analogous angles involving only the Re–P bonds.

In each compound, the bond between the carbonyl group and alkyl substituent (OC–C; C(24)–C(25)) was bent out of the π nodal plane of the free aldehyde. In order to quantify this feature, planes were defined that contained the C⋯O linkages but were perpendicular to the Re–O⋯C planes. The angles of the OC–C bonds with these planes were 19.2° and 19.3°, respectively. The angles of the OC–H bonds with these planes, although somewhat less accurate, were 11.2° and 7.6°. In the corresponding free aldehydes, these angles would be 0°.

The bonds between rhenium and the aldehyde ligand oxygens (2.042(6)–2.066(3) Å) were shorter than those between rhenium and the aldehyde carbons (2.15(1)–2.150(4) Å). Hence, the C⋯O linkage is not bound symmetrically. One consequence is that the perpendicular from rhenium to the C⋯O bond does not intercept the C⋯O midpoint, as illustrated schematically in Chart 2. This feature, which is commonly

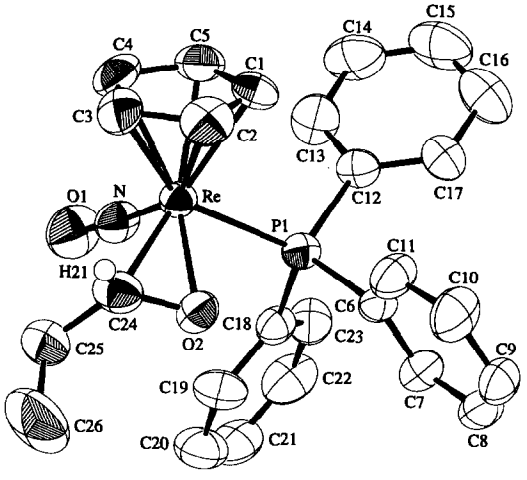

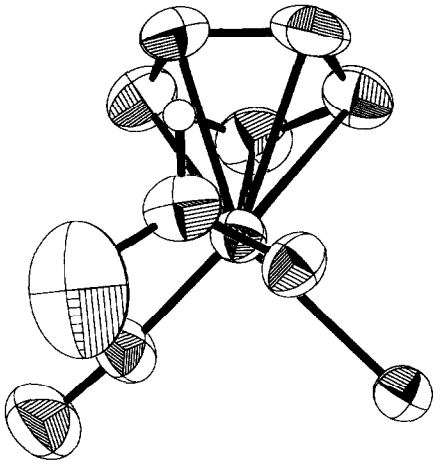

Fig. 1. Structure of the cation of propionaldehyde complex (*RS,SR*)-$[(\eta^5\text{-}C_5H_5)Re(NO)(PPh_3)(\eta^2\text{-}O{=}CHCH_2CH_3)]^+$ PF_6^- ($\mathbf{1b}^+$ PF_6^-): top, numbering diagram; bottom, Newman-type projection with phenyl rings omitted.

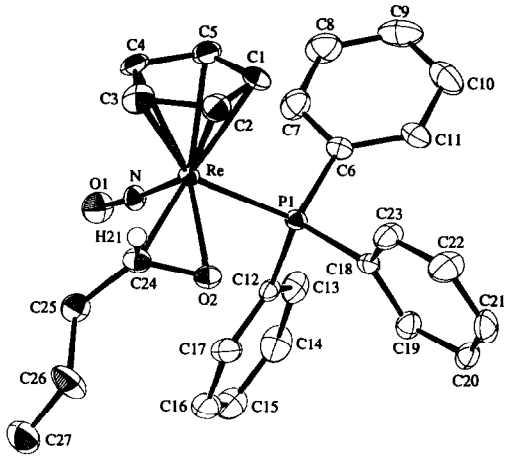

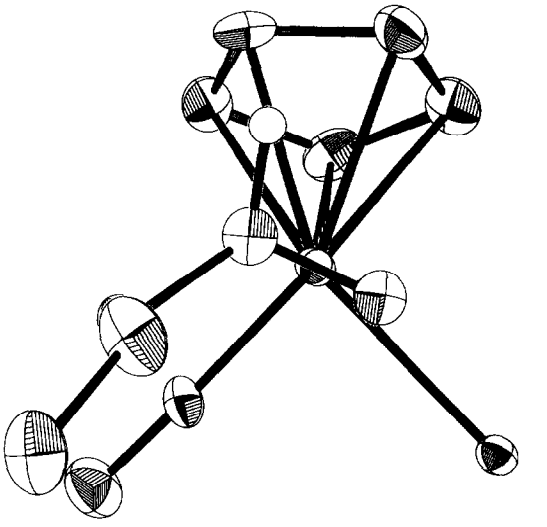

Fig. 2. Structure of the cation of butyraldehyde complex (*RS,SR*)-$[(\eta^5\text{-}C_5H_5)Re(NO)(PPh_3)(\eta^2\text{-}O{=}CHCH_2CH_2CH_3)]^+$ PF_6^- ($\mathbf{1c}^+$ PF_6^-): top, numbering diagram; bottom, Newman-type projection with phenyl rings omitted.

termed "slippage" [14], was quantified by a parameter previously described (Chart 2) [5]. In brief, the slippage parameter value is 0% when the perpendicular intercepts the C⋯O midpoint, and 100% when it passes through the carbon or oxygen atom (∠ Re–O–C or Re–C–O = 90°).

2.2. Synthesis and structure of a pivalaldehyde complex

The substitution-labile dichloromethane complex $[(\eta^5\text{-}C_5H_5)Re(NO)(PPh_3)(ClCH_2Cl)]^+$ BF_4^- ($\mathbf{2}^+$ BF_4^-) was generated as previously reported [15] and treated with excess pivalaldehyde (eqn. (i)). A simple precipitation gave $[(\eta^5\text{-}C_5H_5)Re(NO)(PPh_3)(\eta^2\text{-}O{=}CHC(CH_3)_3)]^+$ BF_4^- ($\mathbf{1g}^+$ BF_4^-) in 81% yield as a tan powder that was nearly analytically pure. The aldehyde ligand in $\mathbf{1g}^+$ BF_4^- was much more labile than those in **1b**, $\mathbf{c}^+$ X^-. In dichloromethane, decomposition occurred to give the previously characterized bridging chloride complex $[(\eta^5\text{-}C_5H_5)Re(NO)(PPh_3)]_2Cl^+$ BF_4^- [15]. This attribute suggests, as is more fully analyzed elsewhere for other labile adducts of **I** [16], a facile equilibrium between $\mathbf{1g}^+$ BF_4^- and $\mathbf{2}^+$ BF_4^-.

TABLE 2. Atomic coordinates and equivalent isotropic thermal parameters of located atoms in $\mathbf{1b}^+$ PF_6^- and $\mathbf{1c}^+$ PF_6^- [a]

	$\mathbf{1b}^+$ PF_6^-				$\mathbf{1c}^+$ PF_6^-			
	x	*y*	*z*	*B* (Å²)	*x*	*y*	*z*	*B* (Å²)
Re	0.22973(4)	0.22342(2)	0.04256(3)	2.955(7)	0.04513(1)	0.22636(1)	0.24485(2)	1.161(5)
P1	0.3489(2)	0.3362(1)	0.0233(2)	3.06(5)	0.02405(8)	0.34040(7)	0.3521(1)	1.20(2)
P2	−0.2085(3)	0.0769(2)	0.0900(2)	4.93(7)	0.0740(1)	0.06965(8)	−0.2080(1)	1.86(3)
F1	−0.307(1)	0.0143(6)	0.0491(8)	8.4(3)	0.0434(2)	0.0126(2)	−0.3288(4)	3.50(8)
F2	−0.098(2)	0.0235(8)	0.115(1)	14.5(5)	0.1056(3)	0.1256(2)	−0.0871(4)	4.27(9)
F3	−0.110(1)	0.1337(7)	0.130(1)	12.8(5)	0.1664(2)	0.0848(2)	−0.2564(4)	3.96(9)
F4	−0.253(1)	0.068(1)	0.1777(8)	12.3(4)	0.0199(3)	−0.0543(2)	0.1611(4)	4.14(9)
F5	−0.180(2)	0.087(1)	−0.0031(9)	15.1(6)	0.0233(3)	0.1305(2)	0.6938(4)	4.4(1)
F6	0.682(1)	0.1280(8)	0.065(2)	15.8(7)	0.1239(3)	0.0075(2)	−0.1116(4)	5.0(1)
O1	−0.0134(8)	0.3051(5)	0.0567(6)	6.0(2)	0.0532(3)	0.3078(2)	−0.0040(4)	2.53(8)
O2	0.2408(6)	0.2207(4)	−0.0931(4)	3.8(1)	−0.0931(3)	0.2210(2)	0.2493(4)	1.72(8)
N	0.0857(8)	0.2736(5)	0.0476(5)	3.9(2)	0.0468(3)	0.2759(2)	0.0951(4)	1.57(9)
C1	0.415(1)	0.1799(6)	0.1411(7)	4.7(2)	0.1463(4)	0.1868(3)	0.4409(6)	2.4(1)
C2	0.368(1)	0.1217(6)	0.0818(9)	5.1(3)	0.0883(4)	0.1302(3)	0.3939(5)	2.3(1)
C3	0.234(1)	0.1054(6)	0.0956(8)	4.7(3)	0.1015(4)	0.1108(3)	0.2603(6)	2.4(1)
C4	0.202(1)	0.1525(6)	0.1624(8)	5.0(3)	0.1681(4)	0.1569(3)	0.2305(5)	2.1(1)
C5	0.313(1)	0.2000(6)	0.1904(7)	4.6(3)	0.1957(4)	0.2050(3)	0.3385(6)	2.1(1)
C6	0.4719(9)	0.3301(5)	−0.0512(6)	3.2(2)	0.1334(3)	0.3819(3)	0.4312(5)	1.6(1)
C7	0.491(1)	0.3875(6)	−0.1061(7)	3.8(2)	0.2008(4)	0.3891(3)	0.3566(6)	2.4(1)
C8	0.588(1)	0.3832(6)	−0.1605(7)	4.3(2)	0.2844(4)	0.4191(4)	0.4089(7)	3.0(1)
C9	0.668(1)	0.3229(7)	−0.1591(7)	4.7(3)	0.3045(4)	0.4443(4)	0.5439(7)	3.3(1)
C10	0.647(1)	0.2644(7)	−0.1033(9)	5.7(3)	0.2375(4)	0.4392(3)	0.6209(6)	3.0(1)
C11	0.549(1)	0.2682(7)	−0.0500(7)	4.7(2)	0.1529(4)	0.4084(3)	0.5648(6)	2.1(1)
C12	0.437(1)	0.3729(5)	0.1323(6)	3.5(2)	−0.0341(3)	0.4059(3)	0.2274(5)	1.3(1)
C13	0.365(1)	0.3851(7)	0.2010(8)	5.0(3)	−0.0014(4)	0.4755(3)	0.2262(5)	2.2(1)
C14	0.426(1)	0.4137(7)	0.2842(8)	5.9(3)	−0.0496(5)	0.5246(3)	0.1326(6)	2.8(1)
C15	0.562(2)	0.4312(7)	0.2972(9)	6.5(4)	−0.1306(4)	0.5042(3)	0.0390(6)	2.9(1)
C16	0.634(1)	0.4208(8)	0.228(1)	6.7(4)	−0.1625(4)	0.4350(4)	0.0418(6)	2.8(1)
C17	0.571(1)	0.3916(7)	0.1442(8)	4.8(3)	−0.1153(4)	0.3859(3)	0.1366(6)	2.4(1)
C18	0.2377(9)	0.4081(5)	−0.0254(6)	3.2(2)	−0.0445(3)	0.3372(3)	0.4802(5)	1.5(1)
C19	0.141(1)	0.3925(6)	−0.1037(8)	4.8(3)	−0.1029(4)	0.3951(3)	0.4920(5)	1.9(1)
C20	0.056(1)	0.4481(7)	−0.1431(8)	5.4(3)	−0.1528(4)	0.3936(3)	0.5955(5)	2.0(1)
C21	0.068(1)	0.5166(6)	−0.1071(8)	5.3(3)	−0.1431(4)	0.3368(3)	0.6847(6)	2.5(1)
C22	0.162(1)	0.5319(6)	−0.0300(9)	5.4(3)	−0.0862(5)	0.2795(4)	0.6712(7)	3.1(1)
C23	0.247(1)	0.4783(6)	0.0094(8)	4.1(2)	−0.0379(4)	0.2803(3)	0.5693(6)	2.3(1)
C24	0.144(1)	0.1723(6)	−0.0845(8)	4.6(3)	−0.0829(4)	0.1744(3)	0.1524(6)	2.0(1)
C25	−0.001(1)	0.1884(8)	−0.1284(8)	5.8(3)	−0.1288(4)	0.1917(3)	0.0033(6)	2.1(1)
C26	−0.022(2)	0.175(1)	−0.226(1)	10.7(6)	−0.2322(4)	0.1764(4)	−0.0253(6)	3.2(1)
C27	–	–	–	–	−0.2825(5)	0.2099(4)	−0.1575(7)	3.4(2)
H21	0.1660	0.1172	−0.0840	5.0	−0.076(5)	0.123(5)	0.198(7)	5.0

[a] Anisotropically refined atoms are given in the form of the isotropic equivalent displacement parameter defined as: $(4/3)[a^2B_{1,1} + b^2B_{2,2} + c^2B_{3,3} + ab(\cos\gamma)B_{1,2} + ac(\cos\beta)B_{1,3} + bc(\cos\alpha)B_{2,3}]$.

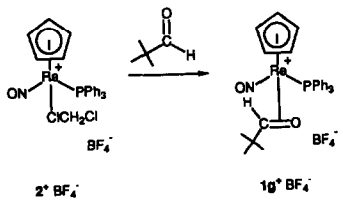

(i)

Complex $\mathbf{1g}^+$ BF_4^- was characterized by IR and NMR (^1H, ^{13}C, ^{31}P) spectroscopies, as summarized in the Experimental section. Solutions were amber colored, similar to other aliphatic aldehyde complexes such as **1b**, $\mathbf{c}^+$ X^-. In contrast, adducts of **I** and aliphatic ketones such as acetone, which exhibit only σ binding modes, give orange solutions and characteristic UV/visible absorptions [6a,7a,c]. Accordingly, $\mathbf{1g}^+$ BF_4^- showed a ^{31}P NMR chemical shift (8.7 ppm, −40°C) in a range characteristic of a π aldehyde complexes (9–11 ppm) [5], and upfield from that associated with σ ketone complexes (18–19 ppm) [6]. Also, the O⎓CH ^1H and ^{13}C NMR chemical shifts (δ 5.40, −40°C; 92.4 ppm, −90°C) were much closer to those of π complexes (δ 5.2–5.4; 60–90 ppm) than σ complexes (δ > 8.40; 214–236 ppm) [6,7a,c].

However, a closer examination of certain spectroscopic properties of $\mathbf{1g}^+$ BF_4^- suggested the possibility of a rapid equilibrium involving a small amount of a σ isomer. For example, the O⎓CH ^{13}C NMR resonance shifted downfield at higher temperatures (98.4 ppm, −40°C; 110.1 ppm, 26°C). The PPh_3 ^{31}P NMR resonance showed a similar but less pronounced effect (8.80 ppm, −40°C; 9.23 ppm, −10°C; 9.75 ppm, 20°C). Also, the otherwise featureless UV/visible spectrum showed a very weak shoulder at 380 nm (CH_2Cl_2, ϵ 700 M^{-1} cm^{-1}; *ca.* 90 M^{-1} cm^{-1} after substraction of UV tail), and a possible weaker shoulder at 328 nm, that were not present in spectra of the corresponding isobutyraldehyde complex $\mathbf{1d}^+$ BF_4^-.

Previous work has established that π/σ equilibria involving aromatic aldehyde complexes of **I** are very temperature and solvent dependent, with proportions of σ isomers increasing at higher temperatures and in less polar solvents [7a,c]. However, $\mathbf{1g}^+$ BF_4^- gave only one IR ν(NO) in dichloromethane at 26°C (1723 cm^{-1}; KBr 1720 cm^{-1}). It fell close to the range associated with π isomers (1740–1729 cm^{-1}), and outside of the range of σ isomers (1697–1680 cm^{-1}). Based upon extinction coefficient data described elsewhere [7a,c], as little as 4% of an absorption due to a second isomer would have been detected. IR spectra of $\mathbf{1g}^+$ BF_4^-, propionaldehyde complex $\mathbf{1b}^+$ BF_4^-, and isobutyraldehyde complex $\mathbf{1d}^+$ BF_4^- were also recorded in the less polar solvent dichloromethane/hexane (60:40 v/v). Under careful conditions, no evidence for σ isomers was observed. However, after extended periods or in the presence of air, some samples gave decomposition products with IR ν(NO) in the 1660–1690 cm^{-1} range.

Finally, low temperature ^{31}P and ^1H NMR spectra of $\mathbf{1g}^+$ PF_6^- were carefully analyzed. Based upon the integration of very small resonances that potentially arise from impurities, an upper bound of 0.5% was placed upon the equilibrium concentration of any π

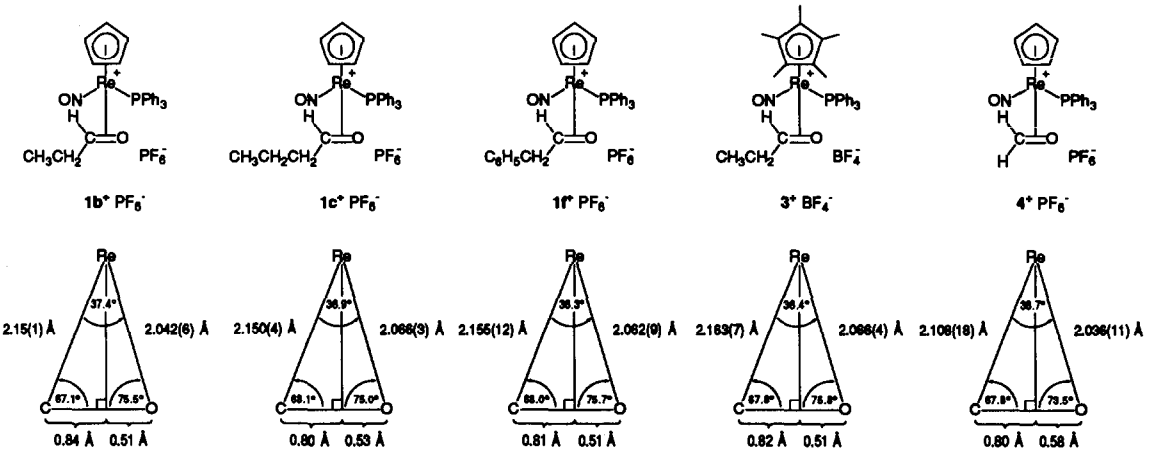

C=O bond	1.35(1) Å	1.338(5) Å	1.318(11) Å	1.325(7) Å	1.374(19) Å
angle, Re-O=C plane with Re-P bond[a]	17.0°	20.5°	22.8°	22.8°	15.0°
slippage[b]	24%	20%	23%	23%	16%
C-R bend-back angle[a,b]	19.2°	19.3°	19.0°	21.0°	-
O=C-C-R' torsion angle	76.8(16)°	77.2(6)°	94.5°	183.6°	-

(a) the software programs utilized do not provide esd's for these data; (b) see text

Chart 2. Views of the Re–O⎓C planes of π aldehyde complexes $[(\eta^5\text{-}C_5R_5)Re(NO)(PPh_3)(\eta^2\text{-}O{=}CHR)]^+$ X^-, and key structural parameters.

TABLE 3. Selected bond distances (Å), bond angles (deg) and torsion angles (deg) in **1b**$^+$ PF_6^- and **1c**$^+$ PF_6^-

	1b$^+$ PF_6^-	**1c**$^+$ PF_6^-
Re–P1	2.437(2)	2.4329(9)
Re–N	1.742(8)	1.766(3)
O1–N	1.19(1)	1.180(4)
Re–O2	2.042(6)	2.066(3)
Re–C24	2.15(1)	2.150(4)
O2–C24	1.35(1)	1.338(5)
C24–C25	1.53(2)	1.532(6)
C24–H21	1.03	1.05(7)
C25–C26	1.45(2)	1.524(6)
C26–C27	–	1.503(7)
Re–C1	2.310(9)	2.310(4)
Re–C2	2.34(1)	2.327(4)
Re–C3	2.30(1)	2.303(4)
Re–C4	2.26(1)	2.269(4)
Re–C5	2.25(1)	2.258(4)
P1–C6	1.820(9)	1.813(4)
P1–C12	1.83(1)	1.821(4)
P1–C18	1.800(9)	1.809(4)
P1–Re–N	89.9(3)	87.0(1)
Re–N–O1	175.2(8)	176.1(3)
Re–O2–C24	75.5(5)	75.0(2)
Re–C24–O2	67.1(6)	68.1(2)
O2–Re–C24	37.4(3)	36.9(1)
O2–C24–C25	120(1)	118.3(4)
O2–C24–H21	119	107(3)
C24–C25–C26	111(1)	110.7(3)
C25–C24–H21	112	126(3)
C25–C26–C27	–	111.7(4)
N–Re–O2–C24	75.9(7)	75.2(3)
P1–Re–O2–C24	162.5(6)	159.1(3)
O2–C24–C25–C26	76.8(16)	77.2(6)
Re–C24–C25–C26	155.9(12)	156.4(4)

diastereomer of the type **III** (Chart 1). A quantitative study of **II**/**III** ratios for a variety of aliphatic aldehyde complexes **1**$^+$ X^- is currently in progress [17].

3. Discussion

The structures of **1b**, **c**$^+$ PF_6^- are compared to those of the phenylacetaldehyde complex **1f**$^+$ PF_6^- and related aliphatic π aldehyde complexes in Chart 2 [6a]. The C⋯O, Re–C, and Re–O bond lengths in **1b**, **c**, **f**$^+$ PF_6^- are identical within experimental error. As expected from commonly accepted π backbonding models, the C⋯O bonds (1.35(1), 1.338(5), 1.318(11) Å) are longer than that in the free ligand propionaldehyde (1.209(4) Å) [18], but shorter than that in 1-propanol (1.41 Å) [19]. All three compounds adopt similar conformations about the OC–CH_2R' bonds, as can be quantified by the O⋯C–C–R′ torsion angles (Chart 2). In all cases, the substituent R′ is distanced away from the bulky rhenium fragment, as is readily seen in Figs. 1 and 2.

The crystal structure of the pentamethylcyclopentadienyl analog of **1b**$^+$ PF_6^-, (*RS,SR*)-$[(\eta^5\text{-}C_5Me_5)Re(NO)(PPh_3)(\eta^2\text{-}O{=}CHCH_2CH_3)]^+$ BF_4^- (**3**$^+$ BF_4^-), has also been determined [9]. Pentamethylcyclopentadienyl ligands are more electron-releasing than cyclopentadienyl ligands [20]. Thus, the increased π basicity of the rhenium fragment in **3**$^+$ BF_4^- might have been expected to give shorter Re–C and Re–O bonds, and a longer C⋯O bond. However, the greater fragment bulk should have an opposite effect. In actuality, the bond distances and angles involving the Re–O⋯C moiety (C⋯O 1.325(7) Å) are essentially identical with those of **1b**, **c**, **f**$^+$ PF_6^- (Chart 2). Curiously, the OC–CH_2CH_3 bond in **3**$^+$ BF_4^- adopts a conformation different from that in **1b**$^+$ PF_6^-, resulting in a methyl group that is antiperiplanar to the C⋯O oxygen.

Alternatively, comparisons can be made with complexes in which the electronic and/or steric properties of the aldehyde ligand have been modified. For example, formaldehyde is a stronger π acid than aliphatic aldehydes [12a], and sterically less demanding. Both factors should enhance backbonding. Accordingly, the Re–C and Re–O bonds in the corresponding π complex $[(\eta^5\text{-}C_5H_5)Re(NO)(PPh_3)(\eta^2\text{-}O{=}CH_2)]^+$ PF_6^- (**4**$^+$ PF_6^-) [4] are shorter than those in **1b**, **c**, **f**$^+$ PF_6^-, whereas the C⋯O bond is longer (Chart 2).

As is summarized in Chart 2, the aldehyde ligands in **1b**, **c**, **f**$^+$ PF_6^- and **3**$^+$ BF_4^- also exhibit remarkably similar slippage values and OC–R bend-back angles. Furthermore, the Re-(O⋯C) conformations are quite close, as evidenced by the angles of the Re–O⋯C planes with the Re–P bonds. The crystal structures of several π aromatic aldehyde complexes $[(\eta^5\text{-}C_5H_5)Re(NO)(PPh_3)(\eta^2\text{-}O{=}CHAr)]^+$ X^- have also been determined [7a, 21]. These exhibit somewhat different structural trends, and will be analyzed in a separate publication. Although Lewis base adducts of a number of coordinatively unsaturated d^6 metal fragments of the type $[(\eta^5\text{-}C_5R_5)M(L)(L')]^+$ have been extensively studied, we are unaware of any other structurally characterized simple mononuclear π aliphatic aldehyde complexes [22].

Although the gross structural properties of pivalaldehyde complex **1g**$^+$ BF_4^- have been defined, several unusual features are evident. First, the NMR data show much more temperature dependence than those of other aliphatic aldehyde complexes **1**$^+$ X^- [7c]. The chemical shift trends suggest a higher equilibrium concentration of a σ isomer. This follows logically from the increased bulk of the C⋯O substituent, which moves to a position remote from the rhenium fragment in the *trans*-σ binding mode. However, less

than 4% of a σ isomer is present in dichloromethane at room temperature, as bounded by IR analysis. More precise equilibrium data would obviously be desirable. However, previous studies have shown that the π and σ isomers of aromatic aldehyde complexes $[(\eta^5\text{-}C_5H_5)Re(NO)(PPh_3)(O{=}CHAr)]^+ X^-$ interconvert at extremely rapid rates. Only in exceptional cases involving σ-biased complexes has it proven possible to decoalesce isomers by low temperature NMR [7b].

Second, the IR ν(NO) of **1g**$^+$ BF_4^- is the lowest observed to date for a π aldehyde complex of the rhenium fragment **I**. We speculate that the large t-butyl substituent effects a greater distortion of the Re-(O=C) conformation from that in the idealized structure **II**. This would diminish backbonding from the d orbital HOMO shown in **I** (Chart 1) to the aldehyde ligand. Consequentially, backbonding to the NO ligand should be increased, giving a lower IR ν(NO). Interestingly, another rhenium π pivalaldehyde complex, the bis(imido) bis(neopentyl) species $Re(=NAr)_2(CH_2C(CH_3)_3)(\eta^2\text{-}O{=}CHC(CH_3)_3)$ (Ar = 2,6-C_6H_3-^{i}Pr), has been reported [23]. It exhibits O=CH ^{1}H and ^{13}C NMR chemical shifts (C_6D_6: δ 4.91; 90.25 ppm) close to those of **1g**$^+$ BF_4^-.

In conclusion, we have established that pivalaldehyde binds to the rhenium fragment **I** in predominantly a π manner (> 96%) in dichloromethane at room temperature. Since aliphatic aldehydes that are bulkier than pivalaldehyde are rare, it can be confidently assumed that essentially all aliphatic aldehydes will give π complexes with **I**. Finally, reliable crystallographic data for such aldehyde complexes are now available. The low temperature structure of **1c**$^+$ PF_6^- is particularly accurate, and the exceptional homology exhibited by **1b**, **c**, **f**$^+$ PF_6^- (Chart 2) affords a statistical confidence level that is greater than that derivable from any single complex. Bonding trends in the corresponding aromatic aldehyde complexes will be the subject of a detailed analysis in the near future.

4. Experimental section

4.1. General data

General procedures were identical to those in a previous paper [5]. Pivalaldehyde and NH_4^+ PF_6^- (Aldrich) were used as received, and **1c**$^+$ PF_6^- was prepared as described earlier [5].

4.2. $[(\eta^5\text{-}C_5H_5)Re(NO)(PPh_3)(\eta^2\text{-}O{=}CHCH_2CH_3)]^+$ PF_6^- (**1b**$^+$ PF_6^-).

This synthesis illustrates an anion metathesis that is general for this series of compounds. A Schlenk flask was charged with **1b**$^+$ BF_4^- (0.0354 g, 0.0514 mmol) [5], NH_4^+ PF_6^- (0.0854 g, 0.524 mmol), acetone (5 ml), and a stir bar. The mixture was stirred for 10 min, and the solvent was removed under oil pump vacuum. The residue was extracted with CH_2Cl_2 (5 ml). The extract was filtered through a medium porosity fritted disk, and concentrated to *ca.* 1 ml. Then ether (25 ml) was added with stirring. The resulting yellow powder was collected by filtration and dried under oil pump vacuum to give **1b**$^+$ PF_6^- (0.0334 g, 0.0447 mmol, 87%). The IR, ^{1}H, and ^{31}P{^{1}H} NMR spectra were identical with those reported previously [5].

4.3. $[(\eta^5\text{-}C_5H_5)Re(NO)(PPh_3)(\eta^2\text{-}O{=}CHC(CH_3)_3)]^+$ BF_4^- (**1g**$^+$ BF_4^-)

A Schlenk flask was charged with $(\eta^5\text{-}C_5H_5)$-$Re(NO)(PPh_3)(CH_3)$ (0.505 g, 0.904 mmol) [24], CH_2Cl_2 (10 ml), and a stir bar, and was cooled to −80°C. Then $HBF_4 \cdot OEt_2$ (130 μl, 1.00 mmol) was added with stirring [15]. After 20 min, pivalaldehyde (0.55 ml, 0.436 g, 5.06 mmol) was added *via* syringe. After 25 min, the cold bath was removed. After 3 h, ether (50 ml) was added, and the resulting tan precipitate was collected by filtration and dried under oil pump vacuum to give **1g**$^+$ BF_4^- (0.526 g, 0.735 mmol, 81%), mp 179–180°C (dec). Anal. Calcd for $C_{28}H_{30}$-BF_4NO_2PRe: C, 46.94; H, 4.22. Found: C, 46.31; H, 4.25%.

IR (cm^{-1}, CH_2Cl_2/KBr): ν(NO) 1723/1720s. NMR (CD_2Cl_2, −40°C): ^{1}H (δ) 7.70–7.38 (m, 3Ph), 5.95 (s, C_5H_5), 5.40 (s, O=CH), 0.70 (s, $3CH_3$); ^{13}C{^{1}H} (ppm) 133.5 (d, J_{CP} 9.6 Hz, *o*-Ph), 132.7 (s, *p*-Ph), 129.6 (d, J_{CP} 11.4 Hz, *m*-Ph), 126.6 (d, J_{CP} 58.1 Hz, *i*-Ph), 98.4 (s, C_5H_5), 92.7 (s, O=C), 38.1 (s, CCH_3), 28.0 (s, $3CH_3$); ^{31}P{^{1}H} (ppm) 8.7 (s).

4.4. Crystal structures

Ether was slowly added by vapor diffusion to CH_2Cl_2 solutions of **1b**$^+$ PF_6^- or **1c**$^+$ PF_6^-. This gave yellow plates that were mounted for data collection on an Enraf-Nonius CAD-4 diffractometer as summarized in Table 1. Cell constants were obtained from 25 reflections (**1b**$^+$ PF_6^-: $10° < 2\theta < 25°$; **1c**$^+$ PF_6^-: $18° < 2\theta < 25°$). The space groups were determined from systematic absences (**1b**$^+$ PF_6^-: $h0l$ $l = 2n$, $0k0$ $k = 2n$; **1c**$^+$ PF_6^-: $h0l$ $h = 2n$, $0k0$ $k = 2n$) and subsequent least-squares refinement. Lorentz, polarization, and empirical absorption (Ψ scans) corrections were applied to the data. The structures were solved by standard heavy-atom techniques with the SDP/VAX package [25]. The O=CH hydrogens were located, and that of **1c**$^+$ PF_6^- was refined with fixed isotropic thermal parameters. The remaining hydrogen atom positions were calculated and added to the structure factor calculations but were not refined. The PF_6^- anion of **1b**$^+$ PF_6^- was

disordered. Scattering factors, and $\Delta f'$ and $\Delta f''$ values, were taken from the literature [26].

5. Supplementary material available

Tables of anisotropic thermal parameters, hydrogen atom atomic coordinates, and calculated and observed structure factors for **1b**, c^+ PF_6^- are available from the corresponding author, and have been deposited with the Cambridge Crystallographic Data Centre.

Acknowledgment

We thank the NIH for support of this research.

References

1 (a) M. Kitamura, S. Okada, S. Suga and R. Noyori, *J. Am. Chem. Soc., 111* (1989) 4028; (b) K. Soai and S. Niwa, *Chem. Rev., 92* (1992) 833.
2 (a) E. J. Corey, *Pure Appl. Chem., 62* (1990) 1209; (b) M. Sawamura and Y. Ito, *Chem. Rev., 92* (1992), 857.
3 (a) B. Schmidt and D. Seebach, *Angew. Chem., Int. Ed. Engl., 30* (1991) 1321; (b) R. O. Duthaler and A. Hafner, *Chem. Rev., 92* (1992) 807.
4 W. E. Buhro, S. Georgiou, J. M. Fernández, A. T. Patton, C. E. Strouse and J. A. Gladysz, *Organometallics, 5* (1986) 956.
5 C. M. Garner, N. Quirós Méndez, J. J. Kowalczyk, J. M. Fernández, K. Emerson, R. D. Larsen and J. A. Gladysz, *J. Am. Chem. Soc., 112* (1990) 5146.
6 (a) D. M. Dalton, J. M. Fernández, K. Emerson, R. D. Larsen, A .M. Arif and J. A. Gladysz, *J. Am. Chem. Soc., 112* (1990) 9198; (b) D. P. Klein, D. M. Dalton, N. Quirós Méndez, A. M. Arif and J. A. Gladysz, *J. Organomet. Chem., 412* (1991) C7; (c) D. M. Dalton and J. A. Gladysz, *J. Chem., Soc., Dalton Trans.*, (1991) 2741.
7 (a) N. Quirós Méndez, A. M. Arif and J. A. Gladysz, *Angew. Chem., Int. Ed. Engl., 29* (1990) 1473; (b) N. Quirós Méndez, C. L. Mayne and J. A. Gladysz, *Angew. Chem., Int. Ed. Engl., 29* (1990) 1475; (c) N. Quirós Méndez, J. W. Seyler, A. M. Arif and J. A. Gladysz, *J. Am. Chem. Soc.*, in press.
8 D. M. Dalton, C. M. Garner, J. M. Fernández and J. A. Gladysz, *J. Org. Chem., 56* (1991) 6823.
9 F. Agbossou, J. A. Ramsden, Y.-H. Huang, A. M. Arif and J. A. Gladysz, *Organometallics, 11* (1992) 693.
10 I. Saura-Llamas, D. M. Dalton, A. M. Arif and J. A. Gladysz, *Organometallics, 11* (1992) 683.
11 Some lead references: (a) W. D. Harman, M. Sekine and H. Taube, *J. Am. Chem. Soc., 110* (1988) 2439.; (b) T. J. LePage and K. B. Wiberg, *J. Am. Chem. Soc., 110* (1988) 6642; (c) J. W. Faller and Y. Ma, *J. Am. Chem. Soc., 113* (1991) 1579; (d) V. Branchadell and A. Oliva, *J. Am. Chem. Soc., 114* (1992) 4357; (e) F. Delbecq and P. Sautet, *J. Am. Chem. Soc., 114* (1992) 2446.
12 Some short reviews: (a) Y.-H. Huang and J. A. Gladysz, *J. Chem. Ed., 65* (1988) 298; (b) S. Shambayati, W. E. Crowe and S. L. Schreiber, *Angew. Chem., Int. Ed. Engl., 29* (1990) 256.
13 (a) T.-S. Peng, A. M. Arif and J. A. Gladysz, *Helv. Chim. Acta, 75* (1992) 442; (b) T.-S. Peng and J. A. Gladysz, *J. Am. Chem. Soc., 115* (1992) 4174.
14 (a) O. Eisenstein and R. Hoffmann, *J. Am. Chem. Soc., 103* (1981) 4308; (b) A. D. Cameron, V. H. Smith, Jr. and M. C. Baird, *J. Chem. Soc., Dalton Trans.*, (1988) 1037.
15 J. M. Fernández and J. A. Gladysz, *Organometallics, 8* (1989) 207.
16 A. Igau and J. A. Gladysz, *Polyhedron, 10* (1991) 1903.
17 B. Boone, unpublished results, University of Utah.
18 P. van Nuffel, L. van den Enden, C. van Alsenoy and H. J. Geise, *J. Mol. Struct., 116* (1984) 99.
19 N. E. A. Aziz and F. Rogowski, *Z. Naturforsch., 19b* (1964) 967.
20 (a) D. L. Lichtenberger and G. E. Kellogg, *Acc. Chem. Res., 20* (1987) 379; (b) J. R. Sowa, Jr. and R. J. Angelici, *J. Am. Chem. Soc., 113* (1991) 2537.
21 D. P. Klein, A.M. Arif, unpublished results, University of Utah.
22 For crystallographically characterized π formaldehyde complexes, see reference 12a. For a molybdenum cyclopentadienyl π-benzaldehyde complex, see: (a) H. Brunner, J. Wachter, I. Bernal and M. Creswick, *Angew. Chem., Int. Ed. Engl., 18* (1979) 861; (b) M. W. Creswick and I. Bernal, *Inorg. Chim. Acta, 71* (1983) 41.
23 I. A. Weinstock, R. R. Schrock, D. S. Williams and W. E. Crowe, *Organometallics, 10* (1991) 1.
24 (a) W. Tam, G.-Y. Lin, W.-K. Wong, W. A. Kiel, V. K. Wong and J. A. Gladysz, *J. Am. Chem. Soc., 104* (1982) 141; (b) F. Agbossou, E. J. O'Connor, C. M. Garner, N. Quirós Méndez, J. M. Fernández, A. T. Patton, J. A. Ramsden and J. A. Gladysz, *Inorg. Syn., 29* (1992) 211.
25 B. A. Frenz, in H. Schenk, R. Olthof-Hazelkamp, H. van Konigsveld and G. C. Bassi (eds.), *Computing and Crystallography*, Delft University Press, Delft, Holland, 1978, pp. 64–71.
26 D. T. Cromer and J. T. Waber, in J. A. Ibers and W. C. Hamilton (eds.), *International Tables for X-ray Crystallography*, Kynoch, Birmingham, England, 1974, Volume IV, pp. 72–98, 149–150; tables 2.2B and 2.3.1.